© Oxford University Press

Experimentation with a transcranial magnetic stimulation system for functional brain mapping

Gil J. Ettinger[1]*, Michael E. Leventon[1], W. Eric L. Grimson[1], Ron Kikinis[2],
Laverne Gugino[3], Wayne Cote[3], Larry Sprung[3], Linda Aglio[3],
Martha E. Shenton[4], Geoff Potts[4], Victor L. Hernandez[5] and Eben Alexander[6]

[1]Artificial Intelligence Laboratory, Massachusetts Institute of Technology, Cambridge, MA, USA
[2]Department of Radiology, Brigham and Women's Hospital, Boston, MA, USA
[3]Department of Anesthesiology, Brigham and Women's Hospital, Boston, MA, USA
[4]Department of Psychiatry, Brigham and Women's Hospital, Boston, MA, USA
[5]Department of EE&CS, Massachusetts Institute of Technology, Cambridge, MA, USA
[6]Department of Neurosurgery, Brigham and Women's Hospital, Boston, MA, USA

Abstract
We describe functional brain mapping experiments using a transcranial magnetic stimulation
(TMS) device. This device, when placed on a subject's scalp, stimulates the underlying neurons
by generating focused magnetic field pulses. A brain mapping is then generated by measuring
responses of different motor and sensory functions to this stimulation. The key process in
generating this mapping is the association of the 3-D positions and orientations of the TMS probe
on the scalp to a 3-D brain reconstruction such as is feasible with a magnetic resonance image
(MRI). We have developed a registration system which not only generates functional brain maps
using such a device, but also provides real-time feedback to guide the technician in placing the
probe at appropriate points on the head to achieve the desired map resolution. Functional areas we
have mapped are the motor and visual cortex. Validation experiments focus on repeatability tests
for mapping the same subjects several times. Applications of the technique include neuroanatomy
research, surgical planning and guidance, treatment and disease monitoring, and therapeutic
procedures.

1. INTRODUCTION

Functional brain mapping, consisting of the association
of motor, sensory and perception functions with different
regions of the brain, is currently an active research area
with applications in surgical guidance, neuroanatomy
research, diagnosis and therapy. Most current non-invasive
techniques for functional brain mapping either sense
biochemical activity in the brain or sense neural activity
directly. Scanners for sensing biochemical activity include
single-photon emission computed tomography (SPECT),
positron emission tomography (PET) and magnetic
resonance imaging (MRI). The ability of these scanners
to capture brain activity results from their sensitivity to
such factors as metabolic rate and blood oxygenation. The
benefit of such scanners is their ability to quickly capture
three-dimensional (3-D) snapshots of the complete brain
activity. They are limited, though, by their high cost and
relatively poor temporal resolution. Direct neural activity
sensing is performed by electroencephalography (EEG)
or magnetoencephalography (MEG). These techniques
achieve fine temporal resolution, but not always fine
spatial resolution. Furthermore, both of these classes of
functional brain imaging rely on passive control of functional

*Corresponding author
(e-mail: ettinger@ai.mit.edu)

Figure 1. Stimulation coil used for TMS mapping.

activation; that is, they image the brain while the subject undergoes an activity aimed at activating the functional area of interest.

Another promising approach to functional brain imaging is the use of a transcranial magnetic stimulation (TMS) device (Cadwell Laboratories Inc., WA, USA and Magstim Company Ltd, England) for actively stimulating different parts of the brain. Such devices, first introduced for stimulating the human motor cortex by Barker *et al.* (1987), consist of a circular or figure-of-eight shaped coil, termed the TMS probe, which can deliver single magnetic field pulse stimuli or pulse trains. An example of a coil is shown in Figure 1. There is no direct electrical contact with the subject—the device works by inducing small electrical currents (estimated at < 0.25 A) in tissue using brief time-varying magnetic pulses that are focused in front of the coil. The peak magnetic fields are similar to those used with MRI scanners. The resulting energy dissipation in tissue is minimal (< 2 J s^{-1}) (Barker *et al.*, 1987). The magnetic field generated by the coil passes through the scalp and skull with little attenuation and causes excitation of cortical neurons. This is one of the main advantages of magnetic stimulation over direct electrical stimulation—electrical impulses are highly attenuated by the skull and therefore can only be used when the brain is directly exposed to accurately localized activities. Magnetic stimulation is also able to penetrate to considerable depths without causing large electrical fields at the surface. As a result, no pain is associated with the stimulations.

We have explored stimulation of both the motor cortex and visual cortex. Excitations in the motor cortex result in

peripheral responses of the affected muscles. Excitations of the visual cortex briefly inhibit interpretation of the affected visual field. The advantages of such a device are:

- Low cost and ease of use—the device is highly portable with few constraints on applicability.
- Active functional activation—rather than trying to spot brain activity when the subject performs different actions, the TMS attempts to directly stimulate certain brain regions and monitor the resulting impact. By using latency measures to track response times, most voluntary responses are eliminated. In principle, this leads to a functional mapping that is highly localized both spatially within the brain and temporally for ease of acquisition.

While research is on-going on the biological implications of such a device, the physics of the generated magnetic field, and the development of psychophysical experiments which gauge brain function, we are exploring the technical problems of converting the locations of TMS probe stimulations and associated muscular–sensory responses to a 3-D functional brain map. The registration of the functional maps to the brain surface is vital for surgical planning, diagnosis and neuroanatomy research applications.

The key steps of our registration problem are:

(i) Register the subject's MRI scan, the subject's position during stimulation and the TMS probe positions/orientations to the same coordinate frame. For maximum accuracy we would like to avoid a fiducial-based system.
(ii) Track the subject's head motion in order to maintain the registration. Head clamps are to be avoided both for the subject's comfort and to allow free access to the whole head region.
(iii) Combine the TMS responses, TMS-to-MRI transform, and head motion to generate a functional brain mapping on any 3-D surface rendered from the MRI scan. Real-time visualization of the current probe pose in the MRI coordinate frame along with an encoding of previously probed locations is to be used to guide the acquisition of subsequent stimulation points. Such guidance avoids redundant probings, reduces acquisition time and supports accurate delineation of 'hot spot' boundaries.

In Ettinger *et al.* (1996) we reported preliminary results of applying a TMS system to mapping the motor cortex. We have since extended the capabilities of the system to simplify the mapping process by providing real-time status feedback, thus allowing us to map a larger number of subjects. We have also extended the application to include the visual cortex and have begun validation experiments for evaluating the
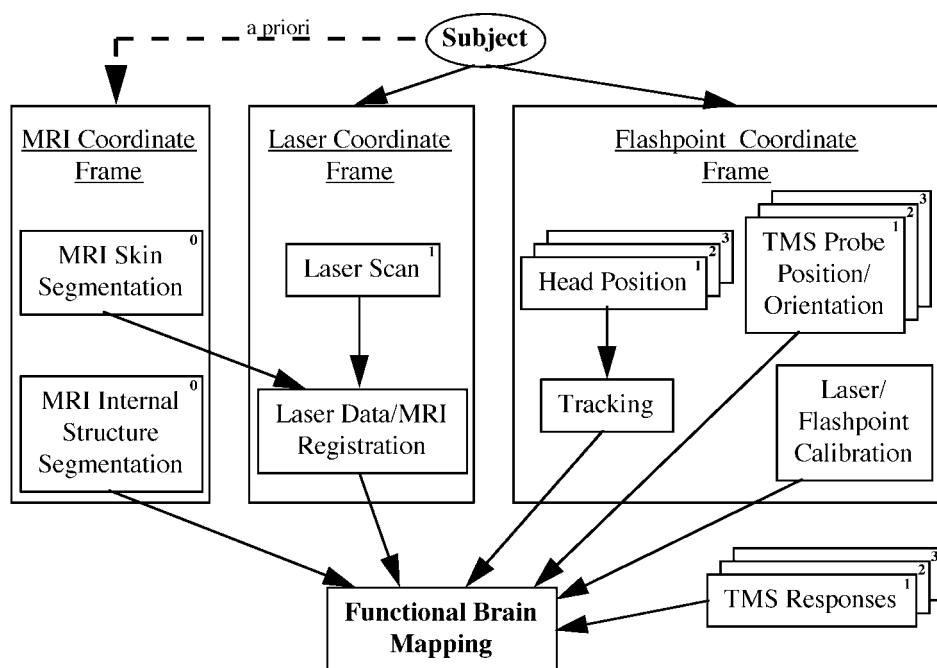
Figure 2. Architecture of the functional brain mapping system.

mapping performance on the motor cortex. We first give a description of our TMS registration/tracking system in Section 2, followed by sample results from the application of our system to mapping the motor and visual cortex in Section 3. Validation test results are described in Section 4.

2. FUNCTIONAL MAPPING SYSTEM

The system we have developed to generate the TMS brain maps is shown in Figure 2. We work with three different coordinate systems:

 (i) **MRI.** The MRI data is captured in the scanner coordinate frame. The data itself is segmented into skin surface for registration and internal structures for brain mapping visualization, all within this coordinate frame.

(ii) **Laser.** The laser scanner provides 3-D data of the subject's scalp surface as positioned for transcranial magnetic stimulation. We use a laser striping triangulation system consisting of a laser unit (laser source and cylindrical lens mounted on a stepper motor) and a camera. The scanner sweeps a plane of laser light across the subject's head and calculates 3-D positions for the laser points that are visible in the camera. Sample laser points scanned on the head of a surgery patient are shown in Figure 3. A prior calibration with a calibration gauge is

performed to calculate the camera parameters and laser plane parameters. The scanning time is about 5 s and the accuracy is about 1 mm at the 1 m stand-off from the scanner which we normally use. Here the coordinate frame of the acquired points is centered at a fixed point within the working volume of the laser system.

(iii) **Flashpoint.** This is a self-contained 3-D tracking system (IGT Inc., CO, USA) consisting of three linear cameras which localize flashing IR LEDs. The system is based on a straightforward triangulation process, in which a point is observed in three orthogonal linear cameras, the positions and orientations of which are known with respect to one another. This active triangulation system is highly reliable, with an accuracy of about 1 mm at the 1 m stand-off from the three linear cameras which we normally use. The system can track a number of LEDs simultaneously. We mount two LEDs on a rod perpendicular to the TMS coil and centered on the middle of the figure-of-eight. This set-up allows specification of the coil's 3-D position and orientation, with twist being the only degree of freedom not currently measured. The magnetic field is focused below the middle of the figure-of-eight. We also tape five LEDs on the subject's scalp for tracking head motion. Redundant LEDs are used for tracking the head position in case motion is great enough
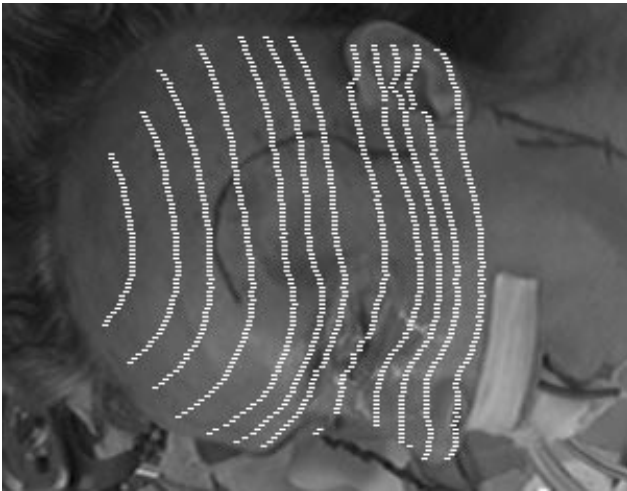
Figure 3. Laser scan of a subject's head. Collected laser points are shown as white curves.

Figure 4. Laser and Flashpoint scanning system.

to block up to two of the LEDs. The position and orientation information returned by the system are represented in a coordinate frame centered at a fixed point within the working volume of the Flashpoint cameras.

The goal of the system is to integrate all of these coordinate systems into a single reference frame; that is, we need to relate sampled TMS probe points to the corresponding points in the MRI scan, which we do by using the laser coordinate system as an intermediary. The laser scanner (laser and its associated camera) and Flashpoint system (three linear cameras) are mounted on the same bar which is attached to a movable arm for ease of placement (see Figure 4). Since we fixate the laser and Flashpoint systems relative to each other, we perform an off-line calibration to obtain the Flashpoint-to-laser transform. This transform is then constant for all subsequent TMS data collections. The transform from laser data to MRI coordinates, though, must be computed for each TMS data collection since it depends on the subject's pose during the mapping session.

2.1. Mapping procedure

A sample data collection procedure, from the perspective of the subject, is:

(i) Acquire an MR image of the subject prior to the TMS session. Segment the scan, using automated techniques by Kapur *et al.* (1995) and Wells (1995) and semi-automated techniques used at Brigham & Women's Hospital, into desired anatomical structures, such as skin, gray matter, white matter, and, if necessary, tumor. Other segmentation techniques may be used as well.
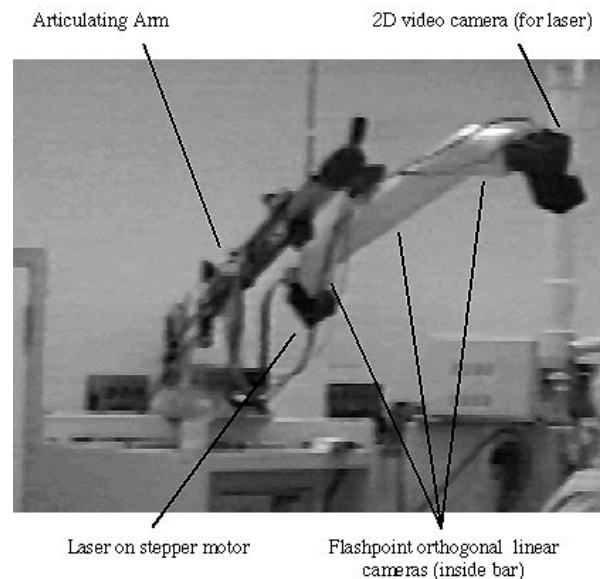
(ii) Set up TMS data collection:

- For motor cortex mapping, place muscle activity sensors on muscles of interest. Muscle activations with latencies of ∼15–30 ms indicate successful stimulation.
- For visual cortex mapping, place the subject in front of a computer screen which will flash sequences of letters in the right and left half of the visual field that the subject will attempt to read. Magnetic stimulation is synchronized to be ∼0.1 s after flashing the letters. False readings indicate successful visual activity suppression.

(iii) Place Flashpoint LEDs on rigid points of the subject's scalp. Currently these are loose LEDs taped in widely separated locations on the skin so that they will not interfere with the TMS probing. For visual cortex mapping we place the LEDs on a tight-fitting swimming cap so that they are visible during stimulation on the back of the head.

(iv) Laser scan the subject—the laser plane is swept across the subject's head collecting 3-D positional data of visible skin surfaces. At the same time the positions of the five LEDs taped to the subject's head are acquired by the Flashpoint system.

(v) Collect TMS data—the TMS probe is placed at various points on the subject's scalp, as in Figure 5. At each

10° initial rotation error. This pose region of convergence increases to about 45° for whole-head coverage in MR-to-MR registration applications. Alternatively, a point-alignment method (Grimson *et al.*, 1996) may be used to automatically generate initial alignment candidates, but at a cost of increased processing.

We refine our initial alignment candidate(s) by minimizing an evaluation function that measures the amount of mismatch between the two data sets. In particular, we sum, for all transformed laser points, a term that is a sum of the distances from the transformed laser point to all nearby MRI points, where the distance is weighted by a Gaussian distribution. If vector ℓ_i is a laser point, vector m_j is an MRI point and $\mathbf{T}$ is a coordinate frame transformation for which we are solving, then the evaluation function for a particular transformation is

$$E_1(\mathbf{T}) = -\sum_i \sum_j e^{-|\mathbf{T}\ell_i - m_j|^2/2\sigma^2}.$$

Because of its formulation, the objective function is quite smooth, and thus facilitates 'pulling in' solutions from moderately removed locations in transformation space. By starting with large σ we achieve a large region of convergence and by gradually decreasing the value of σ we lock in on the well-localized minimum. In order to minimize this evaluation function we use the Davidon–Fletcher–Powell (DFP) quasi-Newton method (Press *et al.* 1992).

As a final step we use a rectified least-squares distance measure to ensure that we have reached an optimal solution and to derive an easily interpreted error measure. We again use DFP to minimize the evaluation function:

$$E_2(\mathbf{T}) = \left[\frac{1}{n} \sum_i \min \left[d_{\max}^2, \min_j |\mathbf{T}\ell_i - m_j|^2 \right] \right]^{1/2}$$

where $d_{\max}$ is a preset maximum distance used to limit the impact of outliers. This second objective function is more accurate locally, since it is composed of saturated quadratic forms. We apply several random perturbations to solutions obtained with this function to search for possibly better nearby solutions. Final values of the $E_2(\mathbf{T})$ error function are about 1.5–2.5 mm using MRI data with a resolution of 0.9375 mm × 0.9375 mm × 1.5 mm. But these RMS errors are not direct measures of registration accuracy. They include contributions of the data sampling rate, data resolution, measurement noise and outlier rate. For example, running the registration on (i) a reference dataset generated by randomly sampling 2000 of the 7000 segmented skin points of a sample segmented MR image and (ii) a test dataset generated by randomly sampling 500 skin points from the same MR image, we achieve an average RMS error of 3.4 mm. But the average worse-case post-registration displacement for any point in the whole image volume is only 1.8 mm.

Figure 5. Subject set-up for TMS stimulation. LEDs mounted on the rod, orthogonal to the coil, track the position and orientation of the coil. LEDs taped to the face are used for tracking head motion.

point, the TMS generates a brief magnetic pulse and the responses from the muscle sensors or subject's view of the computer screen are recorded. The position and orientation of the TMS probe are recorded by the Flashpoint system at the same time. 3-D renderings of the subject's MRI skin superimposed with TMS points are generated during the data collection to chart progress and guide continued stimulations.

2.2. Laser data/MRI registration

The key to achieving high accuracy in this application is the registration of the MRI data with the actual subject. We accomplish this task by aligning skin surface from the MRI data to skin surface from the subject acquired with a laser scanner. Accuracy requirements are relatively high as many of the active brain centers being studied are in the order of a few mm^3 in volume. Thus the overall accuracy, including any tracking errors, should be within ∼1–2 mm, which is generally not much larger than the voxel resolution of the MRI scan.

The basis of the registration algorithm we use has been described previously in Ettinger *et al.* (1994, 1996), Grimson *et al.* (1995, 1996) and Ettinger (1997). The first step is an initial alignment for which we use a coarse manual positioning of the laser data relative to the MRI data. The accuracy requirements for the initial alignment are a function of the data coverage of the laser data. We have shown in Ettinger (1997) that for laser data coverage of about 25% of the whole head, the subsequent registration steps converge from about

Given that this RMS error function is not an accurate measure of deviation from the true pose, we use two visualization methods to verify the registration:

- An overlay of the registered rendered MRI skin surface on a calibrated camera's view of the subject. The alignment of both the bounding contour of the head and internal facial features are evaluated qualitatively in this manner.
- The residual error of the laser points to the MRI skin surface are color-coded and displayed in order to gauge the fit of the data sets. Such a visualization highlights any rotation or translation biases which are present in the solution pose.

2.3. Probe and head tracking

The 3-D position of the TMS probe is obtained directly by tracking the Flashpoint LEDs that are rigidly attached to it. In order to track the head motion we record the reference position of the LEDs taped to the patient's head at the time we perform the laser data–MRI registration. When the TMS probe is stimulated we record the new position of the head-mounted LEDs and compute the transform necessary to return the head to its reference position. This transform is applied to the position/orientation of the TMS probe at the time of the corresponding stimulation in order to apply the laser data–MRI transformation. Since we may have up to five LEDs to track the head we use Horn's closed-form least-squares solution (Horn 1987) for the tracking transform.

2.4. Functional map generation

We combine the registration and tracking data to obtain the functional brain mapping using these transforms:

- $\mathbf{F}_L$, transformation from Flashpoint coordinates to laser coordinates; calibrated *a priori*.
- $\mathbf{L}_M$, transformation from laser coordinates (head at time 1) to MRI coordinates; computed from the dynamic registration procedure.
- $\mathbf{H}_r^t$, transformation of head from time t to reference position at time 1.

We have also collected the following TMS data:

- C_p^t, C_o^t, position and orientation of the TMS coil at time t, $t \in [1, T]$, in Flashpoint coordinates.
- For motor cortex mapping we receive r_j^t, the measured first response of muscle j to stimulation t and w_j^t the latency from stimulation to the response.
- For visual cortex suppression we record the letters the subject saw flashing on the computer screen. The set of letters are separated into left and right fields of view for separating the processing of the two sides by the brain.

In order to compute the brain mapping we need to map the TMS responses to the brain surface using the measured coil positions/orientations and associated transformations. To perform this mapping, for each stimulation t, we process those MRI surface points, $S[i]$, that are sufficiently close to $\mathbf{L}_M\mathbf{F}_L\mathbf{H}_r^t C_p^t$ to have been possibly stimulated by the pulse. For each $S[i]$ we compute the distance, $d^t[i]$, to the line defined by the point $\mathbf{L}_M\mathbf{F}_L\mathbf{H}_r^t C_p^t$ and the orientation $\mathbf{L}_M\mathbf{F}_L\mathbf{H}_r^t C_o^t$. For motor cortex mapping we are currently using a Gaussian weighting function proportional to that distance to 'spread' the response r_j^t to the points $S[i]$. The purpose of this (simple) weighting function is to interpolate across the stimulations to obtain a smooth and visible map on the surface of the cortex or white matter. If we let $map_j^t[i]$ represent the mapping of response j to stimulation t on the selected surface, then $map_j^t[i] = G(d^t[i], \sigma)r_j^t$, with G being the Gaussian weighting function. We then let $map_j[i]$, the composite mapping from all stimulations, be the maximum $map_j^t[i]$ over all t, which are then normalized over i. The exact 3-D location of the excited neurons is not a solved problem. This location is a function of the complex interaction of primary and secondary nerve centers, neuron physiology and magnetic field strength and orientation. On-going research in these areas, such as Rosler *et al.* (1989), Meyer *et al.* (1991), Amassian *et al.* (1992, 1994), Maccabee *et al.* (1993) and Rudiak and Marg (1994), may benefit from the registration techniques we describe.

For visual cortex mapping we treat the responses as binary and thus directly map the points that caused positive suppression in the left and/or right fields of view to the MRI surface points, $S[i]$.

3. MAPPING RESULTS

We have performed the TMS brain mapping on 10 motor mapping subjects and five visual mapping subjects. Three of the subjects were neurosurgery patients. Figure 6 shows two methods for visualizing the motor strip mapping for one of the subjects. One method displays the minimum latency response (above threshold) for all the muscles evaluated, while the other displays the response strength for individual muscles. The responses are localized in their anatomically expected locations. In Figure 6b we see all the stimulations that were collected during the session. Since the stimulation points are visualized in real time, such a display provides feedback for guiding subsequent probes, avoiding redundant probes in no response areas and accurately delineating response boundaries.

Figure 7 shows the results of visual cortex mapping. We see that the visual suppression effects are well localized and separated across the right and left fields of view.
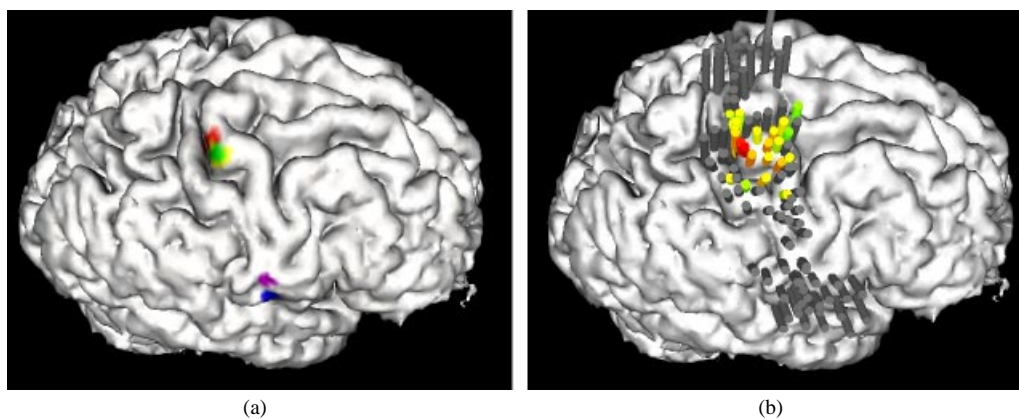
(a)   (b)

Figure 6. (**a**) Motor cortex mapping showing minimum latency response for: index finger (red), forearm (yellow), biceps (green), jaw (blue/purple). (**b**) Oriented stimulation probes color-coded by the response of the index finger muscle. Response strength varies from none to strongest in the order: black, green, yellow, red.
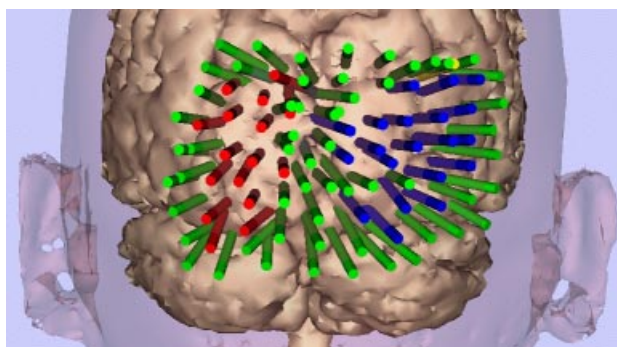

Figure 7. Visual cortex mapping showing stimulation points color-coded by visual suppression response: red = right visual field; blue = left visual field; green = neither.
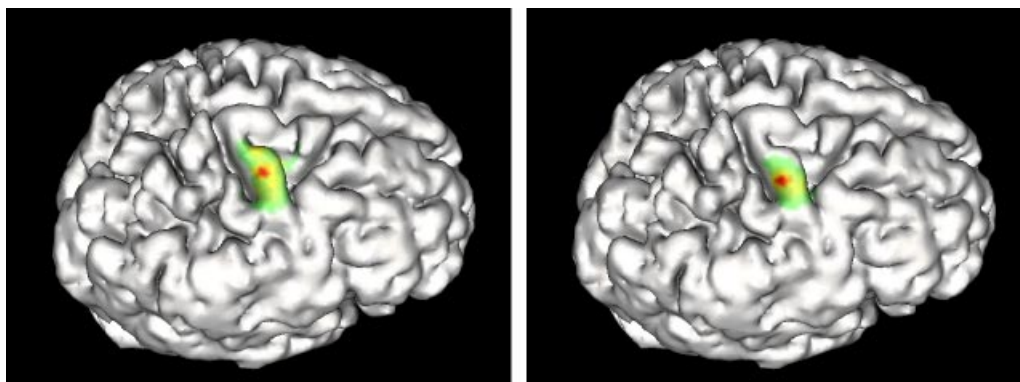

Figure 8. Comparison of the biceps amplitude response mapping of the same subject at two time points.

4. VALIDATION TESTING

Although our functional mappings were received positively by radiology and neurology specialists, it is difficult to validate the results as we have no base functional map for the tested subjects. We are thus pursuing two avenues for validating our results.

- **Map repeatability.** At a minimum we would like to duplicate functional mapping results on the same subject at different points in time. Such results are not definitive indicators of mapping accuracy, but do gauge the reliability of our registration and tracking techniques in the context of functional mapping. We have run such repeatability trials on two subjects in which we mapped the same side of the motor cortex at two different time points. Figure 8 shows the biceps muscle maps generated for one of the subjects at two different times. Initial measurements on distances between minimum latency stimulations of the same muscle resulted in repeatability errors of about 1 cm or less. We are pursuing more accurate methods of evaluating repeatability such as weighting multiple small-latency stimulations by their response amplitudes and using the same stimulation grid pattern which is saved for each subject with his MRI scan.
- **Surgical validation.** An exact validation can be obtained in the operating room in the case of craniotomy surgeries. Surgeons currently use electrical stimulators to directly stimulate the brain surface when they are operating near the motor or sensory cortex. By tracking the position of such stimulators relative to an MR scan on which we have overlaid the functional mapping we can verify the maps. Such tracking in the operating room can be performed using techniques described by Grimson *et al.* (1996) and is planned in the near future.

5. RELATED WORK

Pelizzari *et al.* (1989) have developed a method that matches retrospective data sets (MRI, CT, PET) to one another using a surface-alignment algorithm similar to ours. This work also uses a least-squares minimization of distances between data sets, although with a different distance function and with more operator guidance required. One goal of their work was to register MRI/CT data with PET data to obtain functional mappings. Wasserman *et al.* (1996) used Pelizzari's registration technique for generating functional brain maps from TMS with a reported accuracy of 6 mm. They use a Polhemus magnetic digitizer to collect surface points along the scalp for registration to the MRI skin surface.

Epstein *et al.* (1990), Levy *et al.* (1991) and Meyer *et al.* (1991) have also shown overlaid TMS functional maps on MRI brain surfaces, but the registration was performed using fiducials or stereotactic frames. In other related work, medical researchers (Barker *et al.*, 1987; Amassian *et al.*, 1989; Maccabee *et al.*, 1991; Wassermann *et al.*, 1992; Pascual-Leone *et al.*, 1994) have generated functional maps by essentially drawing grids on the scalp, but did not appear to transfer the maps directly to the cortical surface.

Another 3-D surface registration technique is due to Szeliski and Lavallee (1994). They also perform a least-squares minimization of a distance function to match data sets. Here, the distance is weighted by an estimate of the inverse variance of the measurement noise, and the Levenberg–Marquardt method is used to find the minimum. Once an initial solution is found, points with large errors are removed and the minimization is repeated to refine the pose. They also applied their registration approach to multi-modality registration, in part to obtain functional maps. Other related registration techniques include those of Besl and McKay (1992), Jiang *et al.* (1992), Feldmar and Ayache (1994), Zhang (1994) and Simon (1996).

6. SUMMARY

We have reported on an initial system combining 3-D registration and 3-D tracking techniques to generate functional brain maps from transcranial magnetic stimulation responses. Promising results have been obtained for mapping the motor cortex and visual cortex. Initial validation testing has shown reliable registration and tracking performance. Further testing is ongoing.

The benefits of our approach are:

- No frames, fiducials or head clamps are necessary to maintain accurate registration.
- The position and orientation of the TMS probe is directly tracked instead of relying on probe placement at marked points on the scalp.
- Real-time feedback is provided during the mapping session to identify stimulation points on the cortex.

Such a functional mapping system has applications in:

- Surgical planning—identifying the proximity of tumors to vital functional brain regions.
- Surgical guidance—tracking surgical activity relative to vital functional brain regions.
- Neuroanatomy research—building functional anatomical atlases and correlating functional maps with disease processes.
- Diagnosis—evaluating damage to functional activity of the brain.

- Therapy—using TMS as a therapeutic tool (Belmaker and Fleischmann, 1995) in treating such conditions as depression and akinesa.

7. DESCRIPTION OF THE VIDEO

The video demonstrates a sample TMS session for motor cortex mapping. The system uses a custom-built cart with a configurable laser striping system and Flashpoint tracking system, along with a magnetic stimulation system. Setting up the system consists of: attaching LEDs to the patient's head for tracking by the Flashpoint system; placing electrodes on the muscles to be mapped, and; attaching the TMS coil to a trackable probe.

Once the subject's MRI is registered to the subject's pose, as described in the paper, muscle stimulation proceeds by generating a magnetic field pulse through the coil. Muscle response magnitudes and latencies are measured by the sensing electrodes.

The functional mapping is generated in real-time by tracking in the MRI coordinate frame the position and orientation of the TMS probe as it is placed on the subject's scalp. Two map visualizations are generated: an amplitude response muscle map, showing relative response strength across the brain for specific muscles, and a minimum latency muscle map, showing best temporal responses above threshold for all tested muscles.

REFERENCES

Amassian, V. E., Cracco, R. Q., Maccabee, P. J., Cracco, J. B., Rudell, A. and Eberle, L. (1989) Suppression of visual perception by magnetic coil stimulation of human occipital cortex. *Electroencephalogr. Clin. Neurophysiol*, 74, 458–462.

Amassian, V. E., Eberle, L., Maccabee, P. J. and Cracco, R. Q. (1992) Modelling magnetic coil excitation of human cerebral cortex with a peripheral nerve immersed in a brain-shaped volume conductor: the significance of fiber bending in excitation. *Electroencephalogr. Clin. Neurophysiol*, 85, 291–301.

Amassian, V. E., Maccabee, P. J., Cracco, R. Q., Cracco, J. B., Somasundaram, M., Rothwell, J. C., Eberle, L., Henry, K. and Rudell, A. (1994) The polarity of the induced electric field influences magnetic coil inhibition of human visual cortex: implications for the site of excitation. *Electroencephalogr. Clin. Neurophysiol*, 93, 21–26.

Barker, A. T., Freeston, L. L., Jalinous, R. and Jarratt, J. A. (1987) Magnetic stimulation of the human brain and peripheral nervous system: an introduction and the results of an initial clinical evaluation. *Neurosurgery*, 20, 100–109.

Belmaker, R. H. and Fleischmann, A. (1995) Transcranial magnetic stimulation: a potential new frontier in psychiatry. *Biol. Psychiatry*, 38, 419–412.

Besl, P. and McKay, N. (1992) A method for registration of 3D shapes. *IEEE Trans. PAMI*, 14, 239–256.

Epstein, C. M., Schwartzberg, D. G., Davey, K. R. and Sudderth, D. B. (1990) Localizing the site of magnetic brain stimulation in humans. *Neurology*, 40, 666–670.

Ettinger, G. J. (1997) *Hierarchical Three-Dimensional Medical Image Registration*. Ph.D. Thesis, MIT Department of Electrical Engineering and Computer Science.

Ettinger, G. J., Grimson, W. E. L., Lozano-Pérez, T., Wells III, W. M., White, S. J. and Kikinis, R. (1994) Automatic registration for multiple sclerosis change detection. In *IEEE Workshop on Biomedical Image Analysis*, Seattle, WA, pp. 297–306.

Ettinger, G. J., Grimson, W. E. L., Leventon, M. E., Kikinis, R., Gugino, V., Cote, W., Karapelou, M., Aglio, L., Shenton, M., Potts, G. and Alexander, E. (1996) Non-invasive functional brain mapping using registered transcranial magnetic stimulation. In *IEEE Workshop on Mathematical Methods in Biomedical Image Analysis*, San Francisco, CA, pp. 32–41.

Feldmar, J. and Ayache, N. (1994) Locally affine registration of freeform surfaces. In *IEEE Conf. on Computer Vision and Pattern Recognition*, Seattle, WA, pp. 496–501.

Grimson, W. E. L., Ettinger, G. J., White, S. J., Gleason, P. L., Lozano-Pérez, T., Wells III, W. M. and Kikinis, R. (1995) Evaluating and validating an automated registration system for enhanced reality visualization in surgery. *1st Conference on Computer Vision, Virtual Reality and Robotics in Medicine*, Nice France, pp. 3–12.

Grimson, W. E. L., Ettinger, G. J., White, S. J., Lozano-Pérez, T., Wells III, W. M. and Kikinis, R. (1996) An automatic registration method for frameless stereotaxy, image guided surgery, and enhanced reality visualization. *IEEE Trans. Med. Imag.*, 15, 129–140.

Horn, B. K. P. (1987) Closed-form solution of absolute orientation using unit quaternions. *J. Opt. Soc. Am.* A, 4, 629–642.

Jiang, H., Robb, R. and Holton, K. (1992) A new approach to 3D registration of multimodality medical images by surface matching. *Vision Biomed. Computing*, SPIE Vol. 1808, 196–213.

Kapur, T., Grimson, W. E. L. and Kikinis, R. (1995) Segmentation of brain tissue from MR images. *1st Conference on Computer Vision, Virtual Reality and Robotics in Medicine*, Nice, France, pp. 429–433.

Levy, W. J., Amassian, V. E., Schmid, U. D. and Jungreis, C. (1991) Mapping of motor cortex gyral sites non-invasively by transcranial magnetic stimulation in normal subjects and patients. In Levy, W. J., Cracco, R. Q., Barker, A. T. and Rothwell, J (eds) *Magnetic Motor Stimulation: Basic Principles and Clinical Experience (EEG Suppl. 43)*, pp. 51–75. Elsevier Science Publishers, B.V., Amsterdam.

Maccabee, P. J., Amassian, V. E., Cracco, R. Q., Cracco, J. B., Rudell, A. P., Eberle, L. P. and Zemon, V. (1991) Magnetic coil stimulation of human visual cortex: studies of perception. In Levy, W. J., Cracco, R. Q., Barker, A. T. and Rothwell, J. *Magnetic Motor Stimulation: Basic Principles and Clinical Experience (EEG Suppl. 43)*, pp. 111–120. Elsevier Science Publishers, B.V., Amsterdam.

Maccabee, P. J., Amassian, V. E., Eberle, L. P. and Cracco, R. Q. (1993) Magnetic coil stimulation of straight and bent amphibian and mammalian peripheral nerve *in vitro*: locus of excitation. *J. Physiol.*, 460, 201–219.

Meyer, B. U., Diehl, R., Steinmetz, H., Britton, T. C. and Benecke, R. (1991) Magnetic stimuli applied over motor and visual cortex: influence of coil position and field polarity and motor responses, phosphenes, and eye movements. In Levy, W. J., Cracco, R. Q., Barker, A. T. and Rothwell, J (eds) *Magnetic Motor Stimulation: Basic Principles and Clinical Experience (EEG Suppl. 43)*, pp. 121–134.. Elsevier Science Publishers, B.V., Amsterdam.

Pascual-Leone, A., Gomez-Tortosa, E., Grafman, J., Alway, D., Nichelli, P. and Hallett, M. (1994) Induction of visual extinction by rapid-rate transcranial magnetic stimulation of parietal lobe. *Neurology*, 44, 494–498.

Pelizzari, C., Chen, G., Spelbring, D., Weichselbaum, R. and Chen, C. (1989) Accurate three-dimensional registration of CT, PET, and/or MR images of the brain. *J. Comput. Assis. Tomogr.*, 13, 20–26.

Press, W. H., Teukolsky, S. A., Vetterling, S. T. and Flannery, B. P. (1992) *Numerical Recipes in C, The Art of Scientific Computing* (2nd edn). Cambridge University Press, Cambridge.

Rosler, K. M., Hess, C. W., Heckmann, R. and Ludin, H. P. (1989) Significance of shape and size of the stimulating coil in magnetic stimulation of the human motor cortex. *Neurosci. Lett.*, 100, 347–352.

Rudiak, D. and Marg, E. (1994) Finding the depth of magnetic brain stimulation: a re-evaluation. *Electroencephalogr. Clin. Neurophysiol.*, 93, 358–371.

Simon, D. A. (1996) *Fast and Accurate Shape-Based Registration*. Ph.D. Thesis, Carnegie Mellon University.

Szeliski, R. and Lavallee, S. (1994) Matching 3D anatomical surfaces with non-rigid deformations using octree-splines. In *IEEE Workshop on Biomedical Image Analysis*, Seattle, WA, pp. 144–153.

Wassermann, E. M., McShane, L. M., Hallett, M. and Cohen L. G. (1992) Noninvasive mapping of muscle representations in human motor cortex. *Electroencephalogr. Clin. Neurophysiol.*, 85, 1–8.

Wassermann, E. M., Wang, B., Zeffiro, T. A., Sadato, N., Pascual-Leone, A., Toro, C. and Hallett, M. (1996) Locating the motor cortex on the MRI with transcranial magnetic stimulation and PET. *Neuroimage*, 3, 1–9.

Wells, W. M. (1995) Adaptive segmentation of MRI data. In *1st Conference on Computer Vision, Virtual Reality and Robotics in Medicine*, Nice, France, pp. 59–69.

Zhang, Z. (1994) Iterative point matching for registration of free-form curves and surfaces. *Int. J. Comp. Vision*, 13, 119–152.